Geochemical Perspectives Letters

Apollo 15 green glass He-Ne-Ar signatures - In search for indigenous lunar noble gases

E. Füri, L. Zimmermann, A.E. Saal

Supplementary Information

The Supplementary Information includes:

- Major Element Composition of 15426 Green Glasses
- Noble Gas (He, Ne, Ar) Analysis
- Noble Gas Component Deconvolution and Exposure Ages
- Figures S-1 and S-2
- Tables S-1 and S-2
- Supplementary Information References

Major Element Composition of 15426 Green Glasses

Green glasses collected during the Apollo 15 mission represent quenched picritic (17 to 19 wt. % MgO), very-low-Ti (0.2 to 0.4 wt. % TiO_2) melts, which explosively erupted ~3.4 Gyrs ago by fire-fountaining (*e.g.*, Podosek and Huneke, 1973; Delano, 1979, 1986; Spangler *et al.*, 1984; Steele *et al.*, 1992). They are among the most primitive material yet collected on the Moon (Green and Ringwood, 1973). The green glasses can be divided into discrete compositional groups, which were formed in distinct magmatic events and/or from different source regions (Delano, 1979; Steele *et al.*, 1992).

Table S-1 Average major element composition (in wt. %) of the five compositional groups A-E of Apollo 15426/27 very-low-Ti green glasses.

	Group A	Group B	Group C	Group D	Group E
SiO_2	45.10	46.57	48.17	45.35	45.37
Al_2O_3	7.37	7.62	7.44	7.16	7.15
MgO	17.07	17.65	18.30	17.78	18.41
MnO	0.26	0.26	0.26	0.26	0.26
CaO	8.39	8.51	8.36	8.25	8.04
FeO	19.87	18.74	16.80	20.65	20.33
Na_2O	0.13	0.14	0.11	0.13	0.14
K_2O	0.03	0.03	0.02	0.03	0.03
TiO_2	0.37	0.38	0.23	0.40	0.42
P_2O	0.02	0.03	0.02	0.03	0.03
Cr_2O_3	0.54	0.55	0.58	0.54	0.53
Total	99.14	100.46	100.28	100.59	100.69

Given the small size and mass of the 15426 glass beads studied here, the glasses have not been polished, and their major element composition could not be determined prior to noble gas analyses. However, major element compositions of 15426/27 green glasses were obtained by analyses of over two hundred individual beads using the Cameca SX100 electron microprobe at the Department of Geological Sciences, Brown University (Saal *et al.*, 2008; Wetzel *et al.*, 2015); average compositions for the five compositional groups A-E defined by Delano (1979) are reported in Table S-1.

Noble Gas (He, Ne, Ar) Analysis

Helium, neon, and argon abundances and isotope ratios were determined by CO_2 laser extraction static mass spectrometry (Humbert *et al.*, 2000; Hashizume and Marty, 2004). Twelve 15426 green glass beads, between 13 and 25 (± 2) μg in mass (Table S-2), were loaded into different pits of the laser chamber connected to the purification line of the Helix MC *Plus* (Thermofisher Scientific) noble gas mass spectrometer at the CRPG noble gas analytical facility (Fig. S-1). The sample chamber was pumped to ultra high vacuum and kept at a temperature of 120 °C for ~15 hours. After leaving the samples under high vacuum ($P \leq 10^{-8}$ Torr) for several days prior to analysis, they were heated individually with a continuous-mode infrared CO_2 laser mounted on an *x*-*y* stage. Two heating steps were applied by modulating the power of the laser and monitoring the heating procedure on a TV screen using a CCD camera. A low-temperature step (~600 °C) allowed extracting surface-sited (solar) gases, whereas the fusion step (~1500 °C) was aimed at releasing volume-correlated (cosmogenic, radiogenic, indigenous) noble gas components. The extracted noble gases were purified using five hot (500 °C) and cold (room temperature) Ti sponge getters. Argon was separated from helium and neon by adsorption onto a charcoal finger at 77 K, and helium and neon were subsequently trapped onto a He-cooled cryogenic trap at 15 K. Helium was first released from this trap at 34 K and analysed in peak-jumping mode (^{4}He on the H2 Faraday detector, ^{3}He on the central (Ax) compact discrete dynode (CDD) detector). Neon was released from the cryogenic trap by increasing the temperature to 110 K, and the amount of gas introduced into the mass spectrometer was reduced (to between 50 and 60% of the total amount of neon) through volume dilution in the volume-calibrated purification line (Fig. S-2). The three isotopes of neon were analysed in multi-collection mode (^{22}Ne on H1 CDD, ^{21}Ne on Ax CDD, ^{20}Ne on L2 CDD). Neon isotope analyses consisted of 5 blocks of 30 cycles, and peak centering was performed at the start of each measurement block. Furthermore, a charcoal finger at 77 K and a Zr-Al getter at room temperature were used to minimize the contribution of doubly charged ^{40}Ar and CO_2 to the ^{20}Ne and ^{22}Ne signals, respectively. Given the high mass resolution of the Helix MC *Plus* ($m/\Delta m \approx 1800$), $^{40}Ar^{++}$ is partially resolved from the peak of interest (Honda *et al.*, 2015; Zhang *et al.*, 2016); therefore, no correction was applied to the ^{20}Ne signal. The CO_2^+ signal was measured at the beginning of each neon analysis, and the ^{22}Ne signal was corrected using a CO_2^{++}/CO_2^+ ionization ratio of 0.4 %; notably, the contribution of CO_2^{++} to the ^{22}Ne signal amounted to only ~1 cps, and is therefore negligible. After releasing argon from the charcoal finger, the argon isotopes were analysed in peak-jumping mode (^{40}Ar on the central Faraday detector, ^{38,36}Ar on Ax CDD).

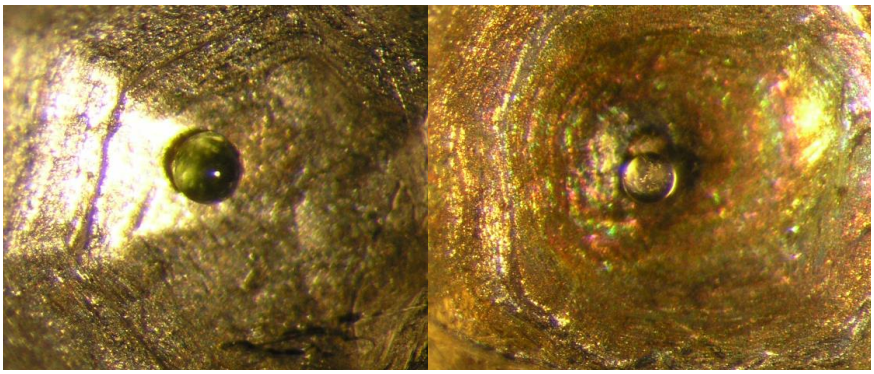

Figure S-1 Glass spherules in laser chamber pits before (left) and after (right) CO_2 laser heating. All glass spherules turned from green to colourless by heating to high temperature.

Air aliquots were used to determine the analytical sensitivity and reproducibility for neon and argon, whereas standard HESJ (He Standard of Japan) of Matsuda *et al.* (2002) with a ^{3}He/^{4}He ratio of 20.63 ± 0.10 R_A (where R_A is the atmospheric ^{3}He/^{4}He ratio) was used as a helium standard. The reproducibility (1σ s.d.) of standard measurements was 4 % for helium and 1 % for neon and argon abundances, whereas the reproducibility of the isotopic ratios ^{20}Ne/^{22}Ne, ^{21}Ne/^{22}Ne, and ^{36}Ar/^{38}Ar was 0.2 %, 0.6 %, and 0.4 %, respectively. Nonetheless, given the very small sample masses analysed here, uncertainties on noble gas concentrations (per gram of sample) are controlled by the precision of the weighing scale (*i.e.* ±2 μg) and are on the order of 8 to 15 %. Procedural blanks,

with the laser off, averaged 2.5 × 10^{-16} mol ^{20}Ne and 2.1 × 10^{-17} mol ^{36}Ar. Helium blanks were below the detection limit. Blank-corrected He-Ne-Ar abundances and isotope ratios for the twelve single 15426 green glass beads are given in Table S-2. Heating steps for which the blank contribution to the measured neon and abundances represents ≥25 % are reported in italics.

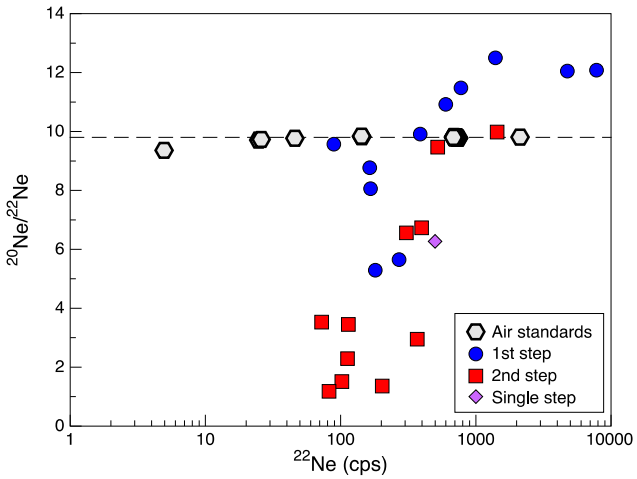

Figure S-2 ^{20}Ne/^{22}Ne ratios (corrected for instrumental mass discrimination) as a function of the ^{22}Ne signals (in counts per second, cps) for air standards and Apollo 15426 green glasses analysed by step-wise heating. The variable count rates for the air standard measurements were obtained by varying the amount of gas introduced into the mass spectrometer through volume dilution in the volume-calibrated purification line. The horizontal dashed line indicates the ^{20}Ne/^{22}Ne ratio of the terrestrial atmosphere (= 9.80 ± 0.08; *e.g.*, Porcelli *et al.*, 2002). Uncertainties (1σ s.d.) are smaller than symbol sizes.

Noble Gas Component Deconvolution and Exposure Ages

For lunar samples that contain a binary mixture between cosmogenic neon and 'trapped' neon implanted by solar wind (SW) irradiation, *i.e.* (^{21,22}Ne$_m$ = ^{21,22}Ne$_{cosm}$ + ^{21,22}Ne$_{tr}$), the amount of cosmogenic ^{21}Ne can be derived from

$$(^{21}Ne)_{cosm} = {}^{22}Ne_m \times \left(\frac{^{21}Ne}{^{22}Ne}\right)_{cosm} \frac{\left(\frac{^{21}Ne}{^{22}Ne}\right)_{tr} - \left(\frac{^{21}Ne}{^{22}Ne}\right)_{m}}{\left(\frac{^{21}Ne}{^{22}Ne}\right)_{tr} - \left(\frac{^{21}Ne}{^{22}Ne}\right)_{cosm}} \qquad \text{Eq. S-1}$$

where (^{22}Ne)$_m$ and (^{21}Ne/^{22}Ne)$_m$ are the measured ^{22}Ne abundances and ^{21}Ne/^{22}Ne ratios, respectively. (^{21}Ne/^{22}Ne)$_{cosm}$ is the cosmogenic neon endmember and (^{21}Ne/^{22}Ne)$_{tr}$ represents trapped SW-derived neon. Neon in the SW has a ^{20}Ne/^{22}Ne and ^{21}Ne/^{22}Ne ratio of 13.78 ± 0.03 and 0.0329 ± 0.0001, respectively (Table S-2; Heber *et al.*, 2009). However, neon implanted into lunar samples by SW irradiation has a significantly lower ^{20}Ne/^{22}Ne value of 11.2 to 12.8 (Grimberg *et al.*, 2006; Péron *et al.*, 2017), consistent with the data obtained here for 15426 green glasses (^{20}Ne/^{22}Ne$_{tr}$ = 12.42 ± 0.05; Fig. 2a). The distinct isotope composition results from both the depth-dependent isotope fractionation upon implantation of SW due to the higher energies and greater penetration depths of heavier isotopes – as demonstrated by Grimberg *et al.* (2006) for the implantation of SW neon into a Genesis target – and the removal of near-surface-sited SW gas by ion sputtering (Wieler *et al.*, 2007; Raquin and Moreira, 2009). In contrast, the neon isotopic signature of the cosmogenic endmember depends on the chemical composition of the sample and the irradiation conditions (*i.e.* solar (SCR) versus galactic cosmic rays (GCR); shielding depth); the (^{21}Ne/^{22}Ne)$_{cosm}$ ratio of mare basalts varies between 0.8 and 0.9 (*e.g.*, Füri *et al.*, 2015), and an average (^{21}Ne/^{22}Ne)$_{cosm}$ value of 0.93 has been reported by Leya *et al.* (2001) for the lunar regolith. Since the irradiation conditions of 15426 green glasses are unknown, and the major element composition of the glass beads studied here has not been determined, we use the lowest (0.035) and highest (0.815) ^{21}Ne/^{22}Ne values measured in our samples for the trapped and cosmogenic endmembers, respectively.

Similarly, the concentration of cosmogenic ^{38}Ar is obtained from

$$(^{38}Ar)_{cosm} = {}^{38}Ar_m \times \frac{\left(\frac{^{36}Ar}{^{38}Ar}\right)_{tr} - \left(\frac{^{36}Ar}{^{38}Ar}\right)_{m}}{\left(\frac{^{36}Ar}{^{38}Ar}\right)_{tr} - \left(\frac{^{36}Ar}{^{38}Ar}\right)_{cosm}} \qquad \text{Eq. S-2}$$

where $(^{38}Ar)_m$ and $(^{36}Ar/^{38}Ar)_m$ are the measured ^{38}Ar abundances and $^{36}Ar/^{38}Ar$ ratios, respectively, $(^{36}Ar/^{38}Ar)_{cosm}$ is the cosmogenic Ar component (≈ 0.7; Hohenberg *et al*., 1978), and $(^{36}Ar/^{38}Ar)_{tr}$ represents trapped SW-derived Ar. SW Ar is characterised by a $^{36}Ar/^{38}Ar$ ratio of 5.47 ± 0.02 (Heber *et al.*, 2009), whereas trapped, surface-correlated Ar in lunar soils generally has a lower isotope ratio of ~5.2 to 5.35 (*e.g.*, Bogard and Hirsch, 1978). The gas-richest sample in this study yields a $^{36}Ar/^{38}Ar$ ratio of 5.51 ± 0.02 at the first heating step; this value is adopted here for trapped argon.

Based on the two-component model, we estimate that for eight out of the twelve glass beads, ≥92 % of the total ^{21}Ne content has been produced in situ by cosmic ray induced spallation reactions during space exposure (Table 1), and the amount of cosmogenic ^{38}Ar represents between 41 and 87 % of the total ^{38}Ar content. The four spherules with the highest measured He-Ne-Ar abundances contain ~33 to 84 % ^{21}Ne of cosmogenic origin with a small fraction (~9 to 25 %) of $^{38}Ar_{cosm}$. Accordingly, the abundance of trapped ^{22}Ne varies between 5 and 61 ($\times 10^{-12}$) mol/g for eight beads, whereas the four gas-rich spherules record $^{22}Ne_{tr}$ concentrations between 189 and 4480 ($\times 10^{-12}$) mol/g. While this trapped component is predominantly extracted at the first heating step – consistent with surface implantation by the SW – the gas-rich glasses release up to 617 ($\times 10^{-12}$) mol$^{22}Ne_{tr}$/g upon sample melting.

The abundance of cosmogenic nuclides in lunar samples depends on the duration of exposure to cosmic rays and the production rates, which themselves are a function of the chemical composition and the irradiation conditions. Given that the lunar regolith is stirred to considerable depths by meteorite impacts, individual soil grains are unlikely to have acquired all their cosmogenic nuclides at a constant depth. Here, we estimate the cosmic ray exposure (CRE) ages by adopting an average production rate for the top 100 g/cm^2 of shielding, and by assuming that contributions from SCRs are negligible. Neon isotope production rates by SCRs are significantly higher than those by GCRs at the uppermost lunar surface (*e.g.*, by a factor ~20 for ^{20}Ne; Hohenberg *et al*., 1978); thus, any contribution of SCR-derived neon is expected to result in a noticeable shift of the $^{21}Ne/^{22}Ne$ ratio to lower values than observed here (≤0.75; Füri *et al.*, 2017). Based on the 2π exposure model of Leya *et al.* (2001), the production rate of cosmogenic ^{21}Ne by GCRs is on the order of 6.7 ± 1.2 ($\times 10^{-14}$) mol(g rock)$^{-1}$ Ma^{-1}, using an averaged composition for the Apollo 15 green glasses (Table S-1). The production rate of cosmogenic ^{38}Ar is less well known (Füri *et al*., 2017). The numerical model of Hohenberg *et al.* (1978) yields a value of 2.5 ± 0.7 ($\times 10^{-14}$) mol(g rock)$^{-1}$ Ma^{-1} for the green glasses, but it significantly underestimates the noble gas nuclide production rates compared to the model of Leya *et al.* (2001). Empirical $^{38}Ar_{cosm}$ production rates from Bogard *et al.* (1971) and Spangler *et al.* (1984) range from 4.1 to 4.5 ($\times 10^{-14}$) mol(g rock)$^{-1}$ Ma^{-1}. We use here the latter values, as they yield CRE ages (T_{38}) that agree, in most cases, within uncertainties with those derived from the $^{21}Ne_{cosm}$ (T_{21}) concentrations (Table 1). We note, however, that new physical models are crucially needed to reliably determine the depth-dependent production rates of cosmogenic argon isotopes in 2π exposure geometries by GCRs.

Table S-2 Helium, neon, and argon abundances and isotope ratios of twelve single Apollo 15426 green glass beads. The isotopic composition of solar wind (Heber *et al.*, 2009), chondritic (*i.e.* A, Q; Busemann *et al.*, 2000, and references therein), and terrestrial (Stuart *et al.*, 2003; Yokochi and Marty, 2004; Péron *et al.*, 2017) noble gases are given for comparison.

Sample ID	Mass (µg)	^{3}He	^{4}He	^{3}He/^{4}He (×10^{-4})	^{20}Ne	^{21}Ne	^{22}Ne	^{20}Ne/^{22}Ne	^{21}Ne/^{22}Ne	^{36}Ar	^{38}Ar	^{40}Ar	^{36}Ar /^{38}Ar
15426-I	25	7.7	3.87	20.0 ± 1.2	174.3	12.8	28.0	6.27 ± 0.02	0.467 ± 0.004	29.3	11.37	*294*	2.54 ± 0.02
15426-II-1	19	2.3	b.d.		65.8	6.7	12.6	5.29 ± 0.02	0.535 ± 0.007	6.6	2.11	b.d.	3.22 ± 0.04
15426-II-2		0.6	b.d.		*17.8*	11.4	14.3	1.36 ± 0.02	0.800 ± 0.012	8.4	9.20	*136*	0.91 ± 0.01
15426-III-1	14	44.1	104.95	4.2 ± 0.2	30368.0	91.9	2520.2	12.05 ± 0.04	0.0370 ± 0.0003	2305.0	436.88	8641	5.32 ± 0.02
15426-III-2		1.9	b.d.		2608.9	50.5	275.7	9.47 ± 0.03	0.184 ± 0.001	775.9	182.41	2367	4.27 ± 0.02
15426-3-1	15	55.6	133.93	4.2 ± 0.2	46605.0	132.9	3863.0	12.08 ± 0.04	0.0350 ± 0.0003	1334.8	243.78	9960	5.51 ± 0.02
15426-3-2		7.5	21.74	3.5 ± 0.2	7088.9	96.7	709.7	9.98 ± 0.03	0.138 ± 0.001	3146.8	650.63	5553	4.83 ± 0.02
15426-2-1	14	4.8	b.d.		*65.5*	1.7	6.9	9.57 ± 0.04	0.257 ± 0.003	10.4	1.90	*71*	5.33 ± 0.08
15426-2-2		5.7	b.d.		*19.8*	6.8	9.3	2.29 ± 0.03	0.738 ± 0.028	6.0	4.66	*197*	1.26 ± 0.02
15426-4-1	21	5.4	b.d.		84.5	2.9	9.7	8.77 ± 0.03	0.301 ± 0.004	12.8	2.58	*54*	4.88 ± 0.04
15426-4-2		0.9	b.d.		*7.2*	4.4	5.5	1.51± 0.04	0.795 ± 0.035	3.8	3.71	*111*	1.10 ± 0.02
15426-5-1	17	3.5	8.60	4.1 ± 0.3	306.1	6.4	31.0	9.91 ± 0.03	0.209 ± 0.002	35.4	7.46	*272*	4.68 ± 0.03
15426-5-2		0.2	b.d.		*26.1*	5.2	7.9	3.45 ± 0.03	0.651 ± 0.023	15.4	6.83	*276*	2.27 ± 0.02
15426-6-1	18	6.0	12.72	4.7 ± 0.3	702.6	6.0	61.0	11.48 ± 0.04	0.100 ± 0.001	67.7	12.85	*969*	5.26 ± 0.02
15426-6-2		2.7	b.d.		82.2	19.3	28.0	2.95 ± 0.04	0.684 ± 0.008	36.9	17.98	*419*	2.06 ± 0.01
15426-11-1	15	3.9	4.67	8.3 ± 0.6	112.9	4.9	14.0	8.06 ± 0.03	0.351 ± 0.005	17.3	3.78	*166*	4.25 ± 0.07
15426-11-2		0.3	b.d.		*16.5*	3.2	*4.9*	3.53 ± 0.05	0.654 ± 0.041	8.6	4.36	*278*	1.94 ± 0.03
15426-10-1	13	13.3	3.51	37.7 ± 9.3	156.1	14.2	27.9	5.65 ± 0.02	0.509 ± 0.007	53.9	12.15	*583*	4.47 ± 0.02
15426-10-2		b.d.	b.d.		*6.3*	5.6	*6.8*	1.18 ± 0.05	0.815 ± 0.047	11.5	9.42	*275*	1.26 ± 0.01
15426-13-1	16	42.4	95.01	4.5 ± 0.3	8191.8	25.7	653.0	12.50 ± 0.04	0.0396 ± 0.0003	566.6	105.56	4395	5.36 ± 0.02
15426-13-2		1.6	5.83	2.7 ± 0.3	170.1	10.5	25.9	6.56 ± 0.02	0.404 ± 0.005	150.3	35.95	*665*	4.21 ± 0.02
15426-12-1	13	30.3	65.04	4.7 ± 0.3	2087.6	24.5	190.4	10.92 ± 0.03	0.130 ± 0.001	252.0	50.07	1805	5.04 ± 0.02
15426-12-2		4.3	12.32	3.5 ± 0.3	284.0	17.4	42.1	6.73 ± 0.02	0.413 ± 0.004	151.4	43.76	*1225*	3.48 ± 0.02

Table S-2 Cont.

Sample ID	Mass (µg)	^{3}He	^{4}He	^{3}He/^{4}He (×10^{-4})	^{20}Ne	^{21}Ne	^{22}Ne	^{20}Ne/^{22}Ne	^{21}Ne/^{22}Ne	^{36}Ar	^{38}Ar	^{40}Ar	^{36}Ar /^{38}Ar
Solar wind				4.64 ± 0.09				13.78 ± 0.03	0.0329 ± 0.0001				5.47 ± 0.01
Q				1.23 ± 0.02				10.11 to 10.67	0.0294 ± 0.0010				5.34 ± 0.02
A				1.35 to 1.55				8.2 ± 0.4	0.025 ± 0.003				5.3 ± 0.1
Earth				≥ 1.26				12.65 to 13.0					5.3

b.d.: below detection limit. Gas extraction steps for which the blank contribution represents ≥25 % are given in italics.
Concentration of ^{4}He in 10^{-9} mol/g, concentrations of ^{3}He, ^{20,21,22}Ne, and ^{36,38,40}Ar in 10^{-12} mol/g.
Uncertainties on noble gas concentrations are on the order of 8 to 15 % for the largest and smallest sample masses, respectively.

Supplementary Information References

Bogard, D.D., Funkhouser, J.G., Schaeffer, O.A., Zähringer, J. (1971) Noble gas abundances in lunar material - Cosmic-ray spallation products and radiation ages from the Sea of Tranquility and the Ocean of Storms. *Journal of Geophysical Research 76*, 2757–2779.

Bogard, D.D., Hirsch, W.C. (1978) Depositional and irradiational history and noble gas contents of orange-black droplets in the 74002/1 core from Shorty Crater. *Proceedings of the 9th Lunar and Planetary Science Conference*, 1981–2000.

Busemann, H., Baur, H., Wieler, R. (2000) Primordial noble gases in "phase Q" in carbonaceous and ordinary chondrites studied by closed-system stepped etching. *Meteoritics and Planetary Science* 35, 949–973.

Delano, J.W. (1979) Apollo 15 green glass: Chemistry and possible origin. *Proceedings of the 10th Lunar Science Conference*, 275–300.

Delano, J.W. (1986) Pristine lunar glasses: criteria, data, and implications. Proceedings of the 16th Lunar and Planetary Science Conference, Part 2, *Journal of Geophysical Research* 91, D201–D213.

Füri, E., Barry, P.H., Taylor, L.A., Marty, B. (2015) Indigenous nitrogen in the Moon: Constraints from coupled nitrogen–noble gas analyses of mare basalts. *Earth and Planetary Science Letters* 431, 195–205.

Füri, E., Deloule, E., Trappitsch, R. (2017) The production rate of cosmogenic deuterium at the Moon's surface. *Earth and Planetary Science Letters* 474, 76–82.

Green, D.H., Ringwood, A.E. (1973) Significance of a primitive lunar basaltic composition present in Apollo 15 soils and breccias. *Earth and Planetary Science Letters* 19, 1–8.

Grimberg, A., Baur, H., Bochsler, P., Bühler, F., Burnett, D.S., Hays, C.C., Heber, V.S., Jurewicz, A.J.G., Wieler, R. (2006) Solar wind neon from Genesis: implications for the lunar noble gas record. *Science* 314, 1133–1135.

Hashizume, K., Marty, B. (2004) Nitrogen isotopic analyses at the sub-picomole level using an ultra-low blank laser extraction technique. In: de Groot, P.A. (Ed.) *Handbook of stable isotope analytical techniques*. Elsevier Science, Amsterdam, 361–375.

Heber, V.S., Wieler, R., Baur, H., Olinger, C., Friedmann, T.A., Burnett, D.S. (2009) Noble gas composition of the solar wind as collected by the Genesis mission. *Geochimica et Cosmochimica Acta* 73, 7414–7432.

Hohenberg, C.M., Marti, K., Podosek, F.A., Reedy, R.C., Shirck, J.R. (1978) Comparison between observed and predicted cosmogenic noble gases in lunar samples. *Proceedings of the 9th Lunar and Planetary Science Conference*, 2311–2344.

Honda, M., Zhang, X., Phillips, D., Hamilton, D., Deerberg, M., Schwieters, J.B. (2015) Redetermination of the ^{21}Ne relative abundance of the atmosphere, using a high resolution, multi-collector noble gas mass spectrometer (HELIX-MC *Plus*). *International Journal of Mass Spectrometry* 387, 1–7.

Humbert, F., Libourel, G., France-Lanord, C., Zimmermann, L., Marty, B. (2000) CO_2-laser extraction-static mass spectrometry analysis of ultra-low concentrations of nitrogen in silicates. *Geostandard Newsletters* 24, 255–260.

Leya, I., Neumann, S., Wieler, R., Michel, R. (2001) The production of cosmogenic nuclides by galactic cosmic-ray particles for 2π exposure geometries. *Meteoritics and Planetary Science* 36, 1547–1561.

Matsuda, J., Matsumoto, T., Sumino, H., Nagao, K., Yamamoto, J., Miura, Y., Kaneoka, I., Takahata, N., Sano, Y. (2002) The ^{3}He/^{4}He ratio of the new internal He Standard of Japan (HESJ). *Geochemical Journal* 36, 191–195.

Péron, S., Moreira, M., Putlitz, B., Kurz, M.D. (2017) Solar wind implantation supplied light volatiles during the first stage of Earth accretion. *Geochemical Perspective Letters* 3, 151–159.

Podosek, F.A., Huneke, J.C. (1973) Argon in Apollo 15 green glass spherules (15426): ^{40}Ar-^{39}Ar age and trapped argon. *Earth and Planetary Science Letters* 19, 413–421.

Porcelli D., Ballentine C.J., Wieler, R. (2002) An overview of noble gas geochemistry and cosmochemstry. In: Porcelli, D., Ballentine, C.J., Wieler, R. (Eds.) *Noble gases in Geochemistry and Cosmochemistry*. Reviews in Mineralogy and Geochemistry, vol. 47. Mineral. Soc. Am., Washington, DC, 1-18.

Raquin, A., Moreira, M. (2009) Atmospheric ^{38}Ar/^{36}Ar in the mantle: Implications for the nature of the terrestrial parent bodies. *Earth and Planetary Science Letters* 287, 551-558.

Saal, A.E., Hauri, E.H., Lo Cascio, M., Van Orman, J.A., Rutherford, M.C., Cooper, R.F. (2008) Volatile content of lunar volcanic glasses and the presence of water in the Moon's interior. *Nature* 454, 192–195.

Spangler, R.R., Warasila, R., Delano, J.W. (1984) ^{39}Ar-^{40}Ar ages for the Apollo 15 green and yellow glasses. Proceedings of the 14th Lunar and Planetary Science Conference, Part 2, *Journal of Geophysical Research* 89, B487–B497.

Steele, A.M., Colson, R.O., Korotev, R.L., Haskin, L.A. (1992) Apollo 15 green glass: Compositional distribution and petrogenesis. *Geochimica et Cosmochimica Acta* 56, 4075–4090.

Stuart, F.M., Lass-Evans, S., Fitton, J.G., Ellam, R.M. (2003) High ^{3}He/^{4}He ratios in picritic basalts from Baffin Island and the role of a mixed reservoir in mantle plumes. *Nature* 424, 57–9.

Wetzel, D.T., Hauri, E.H., Saal, A.E., Rutherford, M.J. (2015) Carbon content and degassing history of the lunar volcanic glasses. *Nature Geoscience* 8, 755–758.

Wieler, R., Grimberg, A., Heber, V.S. (2007) Consequences of the non-existence of the "SEP" component for noble gas geo-and cosmochemistry. *Chemical Geology* 244, 382–390.

Yokochi, R., Marty, B. (2004) A determination of the neon isotopic composition of the deep mantle. *Earth and Planetary Science Letters* 225, 77–88.

Zhang, X., Honda, M., Hamilton, D. (2016) Performance of the High Resolution, Multi-collector Helix MC Plus Noble Gas Mas Spectrometer at the Australian National University. *Journal of The American Society of Mass Spectrometry* 27, 1937–1943.